

Temperature Dependence of Positron Annihilation Lifetimes in High Permeability Polymers: Amorphous Teflons AF

Michael Rudel,[†] Jan Kruse,[†] Klaus Rätzke,^{*,†} Franz Faupel,[†] Yuri P. Yampolskii,[‡] Victor P. Shantarovich,[§] and Günter Dlubek^{||}

Faculty of Engineering, Christian-Albrechts University of Kiel, Kiel, Germany, A. V. Topchiev Institute of Petrochemical Synthesis, Russian Academy of Sciences, Moscow, Russia, N. N. Semenov Institute of Chemical Physics, Russian Academy of Sciences, Moscow, Russia, and ITA Institute for Innovative Technologies, Köthen/Halle, Wiesenring 4, D-06120 Lieskau, Germany

Received July 13, 2007; Revised Manuscript Received November 27, 2007

ABSTRACT: The microstructure of the free volume and its temperature dependence were studied for amorphous Teflon AF 1600 ($T_g = 160\text{ }^\circ\text{C}$) and AF 2400 ($T_g = 240\text{ }^\circ\text{C}$). These copolymers consist of tetrafluoroethylene and 2,2-bis(trifluoromethyl)-4,5-difluoro-1,3-dioxole units and are used as highly permeable membrane materials. We employed positron annihilation lifetime spectroscopy (PALS) to investigate the free volume. From the lifetime spectra analyzed with the routine LT9.0 the hole size distribution, its mean size and width were calculated. Results obtained from a three and a four component analysis of lifetime spectra are compared. Both polymers show very large orthopositronium lifetimes τ_3 (corresponding to large hole sizes) and glass transitions in τ_3 near the expected values. AF 2400 shows an unusual behavior characterized by a nonlinear temperature dependence of the orthopositronium lifetime, extraordinarily large mean values of τ_3 and the widths of the lifetime distributions σ_3 . Possible explanations for this will be discussed in relation to the microstructure of the copolymer.

1. Introduction

In the last 2 decades, positron annihilation lifetime spectroscopy (PALS) has become a generally accepted and most reliable experimental tool for probing the free volume in glassy polymers.^{1–4} When positrons emitted from a radioactive atom (most commonly ^{22}Na) hit condensed matter (in this case a polymer), they slow down quickly. Consecutively, until annihilation, they can exist in the form of free positrons (e^+) or as hydrogen-like Positronium atoms (Ps), the bound state of e^+ (positron) and e^- (electron). Depending on the spins of electron and positron, they can form para-Ps (p-Ps, antiparallel spins of e^+ and e^-) and ortho-Ps (o-Ps, parallel spins). In p-Ps, the selection rule does not prevent rapid intrinsic annihilation, so very short lifetimes (0.125 ns) are observed. Free positrons annihilate with intrinsic lifetimes of about 0.4 ns. Much longer lifetimes are characteristic for annihilation of o-Ps. In vacuum, the intrinsic lifetime of this bound state is 142 ns. However, in matter a coupling of wave functions of o-Ps and electrons of the atoms of the material that surrounds the o-Ps is possible, so the lifetimes are shortened by 2 orders of magnitude. In common conventional glassy polymers, they are in the range of 1.5–3.0 ns.^{5–7} The paradigm of the PALS method is that o-Ps in polymers is localized in regions with reduced density (free volume elements or FVE) and survives there until annihilation: The larger size of the FVE is, the longer the o-Ps lifetime will be. The mathematical expression of this statement is the well-known semiempirical equation, originally developed by

Tao,⁸ and for the first time applied to polymers by Eldrup and co-workers.⁹

$$\tau_{o-Ps} = \frac{1}{2} \left[1 - \left(\frac{R}{R_0} \right) + \frac{1}{2\pi} \sin \left(\frac{2\pi R}{R_0} \right) \right]^{-1} \text{ ns} \quad (1)$$

where τ_{o-Ps} is o-Ps lifetime, R is the corresponding radius of spherical FVE, and $R_0 = R + \Delta R$ (where the adjustable parameter ΔR is 1.66 Å as determined by Jean).¹⁰ This formula predicts a nearly parabolic increase in τ_3 when the hole radius increases, and it can also be applied for hole size distributions.

Since the 90s, the studies of highly permeable glassy polymers, potential or actual membrane materials, indicated that in many such polymers the o-Ps lifetimes are, however, much longer^{11–14} and are in the range of 6–8 ns or even more. For very large holes, the intrinsic o-Ps annihilation rate $\lambda_7^0 = 0.7 \times 10^7 \text{ s}^{-1}$ cannot be neglected and will be taken into account by simple addition. Statistical treatments of the primary PALS experimental data using both finite term methods (e.g., PATFIT) or continuous lifetime distributions (CONTIN or MELT) have been conducted by numerous authors, who studied such high permeability and large free volume polymers. Many of them came to the conclusion that a better statistical fit is obtained, if the lifetime distribution (and FVE size distribution that results from it) is described not by a monomodal Gauss type function but by a bimodal or even multimodal distribution function.^{11–15} However, some doubts on the reliability of such analysis have been raised in the literature.^{16–18} Large hole sizes and multimodal size distributions have also been reported for other materials—polymer sorbents, zeolites, etc. It can be also added that the sizes of FVE found via the PALS experiments have obtained a very reasonable confirmation from other, independent probe methods—inverse gas chromatography,⁴ ^{129}Xe NMR¹⁹ and BET adsorption studies of high free volume materials. Some indication of a bimodal size distribution in a highly permeable polymer was obtained via the two-dimensional ^{129}Xe NMR

* Corresponding author. Technische Fakultät der CAU, Kaiserstrasse 2, 24143 Kiel, Germany. Telephone: +49-431-880-6227. Fax: +49-431-880-6229. E-mail: kr@tf.uni-kiel.de.

[†] Faculty of Engineering, Christian-Albrechts University of Kiel.

[‡] A.V. Topchiev Institute of Petrochemical Synthesis, Russian Academy of Sciences.

[§] N.N. Semenov Institute of Chemical Physics, Russian Academy of Sciences.

^{||} ITA Institute for Innovative Technologies, Köthen/Halle.

method.²⁰ We will discuss this very interesting issue of the type of lifetime and FVE size distribution in polymers and in the later part of this paper.

o-Ps lifetimes (and correspondingly the FVE sizes calculated from them) are very sensitive to the polymer structure, presence of additives, mechanical stress, and other conditions of the experiments such as pressure and temperature.^{10,21–24} Of special interest here are the temperature effects on the o-Ps lifetimes τ_3 . Temperature dependences of τ_3 have been reported for a large number of polymers both below and above their respective glass transition temperatures (see e.g., refs 5–7, 21–23, and 25–28). Such dependence combined with the dilatometric curves (temperature dependence of the specific volume V_{sp} of polymers) found a very useful application: determination of the FVE number density N (or hole number density).^{22,23,27,29,30} Initially it was assumed that the values of N are proportional to the intensity I_3 or statistical weight of the long-lived component in the lifetime spectrum.³¹ However, later it was shown that the intensity also depends on the interaction of Ps precursors with shallow or deep traps, for example, caused by irradiation³² (I_3 is the o-Ps yield), and the aforementioned proportionality holds only for polymer series of similar structure.³³ Combination of $\tau_3(T)$ and $V_{sp}(T)$ curves for various polymers resulted in a relevant finding: the hole number densities N are confined in a rather narrow range of $(1–10) \times 10^{20} \text{ cm}^{-3}$ independent of the polymer nature and structure.^{4,22,23,27,29,30} When this work was conceived, all the reported $\tau_3(T)$ data had been obtained for conventional glassy polymers, such as polyvinyl acetate, polystyrene or poly(methyl methacrylate). Unfortunately, only few results were available for highly permeable polymers, which draw much attention now as advanced materials for gas separation membranes.^{12,34}

Amorphous Teflons AF 1600 and AF 2400 are random copolymers of tetrafluoroethylene and 2,2-bis(trifluoromethyl)-4,5-difluoro-1,3-dioxole with the mole content of $-\text{C}_2\text{F}_4-$ units of 35 and 13%, respectively. They have attracted much attention because of many unusual properties:³⁵ low density (1.7 g/cm^3), much smaller than that of polytetrafluoroethylene (2.1 g/cm^3), attractive optical and dielectric properties, good mechanical characteristics, and very high gas permeabilities.^{35–38} Interestingly, those high gas permeabilities of these polymers are combined with low heat conductivities.³⁵

PAL spectra of perfluorinated polymers had been measured several times at room temperature, also by some of the present authors.^{27,38–41} The data treatment in those publications involved PATFIT and/or CONTIN programs. In the case of the Teflon AF copolymers four component lifetime distributions—corresponding to bimodal size distributions of FVEs—gave better fits than simple three component fits. It should be noted that, under the assumption of a four component fit, the shorter orthopositronium lifetime τ_3 revealed a relatively small intensity I_3 (in the range 2–8%). The present study was prompted by previous results of one of us (GD) which could cast some doubts whether a four component description gives an adequate representation of the FVE size distributions of real polymer materials. By analyzing computer generated spectra, one of us has shown that in the case of a rather broad o-Ps lifetime distribution the routines CONTIN and MELT deliver a bimodal distribution as an artifact of the data analysis (for details see the extended analysis and discussions in refs 16–18). Two narrow peaks appear in the analysis which are located right and left of the maximum of the simulated broad distribution. This artificial splitting may also appear for not so broad distributions when the quality of the experiments (time resolution, statistical

accuracy) is distinctly improved. It was found that it cannot be decided whether the analyzed bimodal distributions come from true bimodal or broad monomodal distributions.^{16–18} It should be noted, however, that the results described in refs 16–18 were obtained for conventional glassy polymers such as polycarbonate, and have never been tested for high free volume polymers like poly(trimethylsilyl propyne) or Teflon AF copolymers.

So the aim of this work was to study the temperature dependence of positron lifetime spectroscopy for amorphous Teflons AF 1600 and AF 2400, both being well investigated high-free volume polymers, in order to find an adequate description of free volume distribution and its temperature dependence above and below their caloric glass transition temperatures.

In the second part of our work now under preparation and to be published in a follow-up paper, we will present a full set of PVT experiments on AF 1600 and AF 2400. We will analyze these data with the help of the Simha-Somcynsky equation of state, calculate the fraction of free volume holes, and compare these results with the hole sizes calculated from the current PALS data in order to estimate the hole densities. Here we will also compare the results for AF 1600 and AF 2400 with those for the cyclic copolymer glass CYTOP and with the linear fluoroelastomer PFE.

2. Experimental Part

2.1. Materials. As already mentioned, two amorphous Teflons AF were studied—the copolymer of 2,2-bis(trifluoromethyl)-4,5-difluoro-1,3-dioxole and tetrafluoroethylene with the content of the former being 87 mol % (AF 2400) and the copolymer with this content being 65% (AF 1600). The films of the two copolymers were cast from solutions in perfluorotoluene in the laboratory of one of the authors.

Differential scanning calorimetry (DSC) was performed with a DSC Q 1000 (TA Instruments) with a heating rate of 10 K/min. In the first heating scan the curves of the as-received polymer samples showed glass transitions at 119 (AF 1600) and $\sim 200^\circ\text{C}$ (AF 2400), which shifted to 153 and 232°C , respectively, in the second heating run. This behavior may be attributed to the desorption of the solvent used in casting. After the samples were dried for a longer period in a vacuum at temperatures above the expected T_g , the glass transitions were found at 160 and 237°C (second heating scan), respectively. These values correspond to those indicated by the provider (DuPont CO).³⁵

2.2. PALS Measurements. Positron annihilation experiments have been performed in a fast–fast coincidence setup with a home made temperature-controlled sample holder under high vacuum conditions as described in more detail, e.g., in 42. Polymeric thin films were cut into $9 \times 9 \text{ mm}^2$ pieces and stacked together with a ^{22}Na source in a sandwich like manner (total thickness = 1 mm) to ensure complete absorption of the positrons in the sample. The sandwich was wrapped into Al-foil and put into the sample holder. Spectra were recorded with up to 10^7 counts within 12 h typically. The temperature was increased and decreased in steps of 10 K (accuracy of temperature $\pm 2 \text{ K}$) using an electrically resistive heater.

3. Results and Discussion

3.1. Positron Lifetime Spectrum at Room Temperature and Its Interpretation. Before discussing the temperature dependence, a suitable model for the description of the data (lifetime τ or the reciprocal, the decay rate λ) and the free volume distribution at room temperature was determined. For the spectrum analysis, we use the new routine LifeTime⁴³ in its last version 9.0.⁴⁴ The routine LT9.0 was developed based on experiences with the routine CONTIN and assumes from the beginning that the distributions of $\alpha_i(\lambda)$ follow a logarithmic Gaussian function, where $\alpha_i(\lambda)$ is the probability density function

Table 1. Parameters of the Lifetime Spectrum of AF 2400 at 30 °C Obtained from Fits under Different Assumptions.
(usually $I_1/I_3 = 1/3$ and $\sigma_1 = 0$)^c

quantity	χ^2/df	τ_1 (ns)	σ_1 (ns)	τ_2 (ns)	σ_2 (ns)	τ_{31} (ns)	σ_{31} (ns)	τ_3 or τ_{32} (ns)	σ_3 or σ_{32} (ns)	P (%)	F_1 (%)	F_{31} (%)	F_3 or F_{32} (%)
a	2.783	0.0927	0	0.3929	0	0	0	6.841	0	22.48	25	0	75
b	1.469	0.0911	0	0.3848	0	0	0	7.069	3.624	24.22	25	0	75
c	0.996	0.1082	0	0.3960	0.1050	0	0	7.276	2.753	22.61	25	0	75
c-free	0.995	0.1063	0.0003	0.3960	0.1045	0	0	7.275	2.755	22.63	25.04	0	74.96
d	0.991	0.1078	0	0.3934	0.0978	2.04	0.002	7.437	2.477	23.08	25	4.50	70.50
d-free	0.991	0.1094	0.01	0.3937	0.0948	1.87	0.026	7.421	2.496	23.55	26.12	4.43	69.45
e-discr	1.018	0.173	0	0.422	0	2.97	0	8.06	35.9	51.0	12.1	36.9	
error \pm^a		0.005	0	0.003	0.002	0	0	0.01	0.01	0.3	0	0	0
error \pm^b		0.01	0	0.01	0.005	0.5	~1	0.3	0.4	0.5	0	1	1

^a Statistical error for analysis c. ^b Statistical error for analysis d. The values 0, 25, and 75 are parameters fixed during the fit. ^c Assumptions: (a) three components, additional constraints: $\sigma_2 = \sigma_3 = 0$ (discrete three term analysis); (b) three components, additional constraint: $\sigma_2 = 0$; (c) three components, no further constraints; (d) four components, here: $I_1/(I_{31} + I_{32}) = 1/3$ and $\sigma_1 = 0$, no further constraints. c-free and d-free denote fits without any constraints. For comparison e-discr shows the results of the unconstrained discrete ($\sigma_1 = \sigma_2 = \sigma_3 = \sigma_4 = 0$) four term analysis. P is the Ps yield given by $P = I_1 + I_3$ (three components) and $P = I_1 + I_{31} + I_{32}$ (four components), respectively. The F_i are the fractions of the Ps components defined by $F_i = I_i/P$.

(pdf) of the annihilation rate of the decay channel i . One of us found recently that employing LT9.0 the artifacts of the spectrum analysis discussed above can be avoided.²⁶ The LT9.0 analysis reproduces very accurately the input-parameters used in the computer generation of spectra. The reason for its success lies in the significant reduction of the degrees of freedom in LT9.0 compared with the routines CONTIN and MELT by assuming the number of different annihilation channels and the shape of the annihilation rate distributions. Of course, similar to the discrete term analysis, we have to test how many components (three or four) describe correctly the lifetime spectrum. However the advantage of LT9.0 is to allow all, or some of them, to follow a distribution in their lifetimes τ_i . The parameter set of the decay function with the minimum number of components, which shows an excellent fit to the experimental spectrum, should be considered as that reasonable result which can be derived from the experiment within the limits of the experimental accuracy. A further increase in the number of components assumed in the spectrum decomposition may be possible, but would not be required and therefore not supported by the experiment. (See the general discussion of the problem of deconvolution and lifetime extraction for nonexponential decays in ref 45.)

The program LT9.0 expresses the lifetime spectrum by the continuous function

$$s(t) = \sum_{i=1,2,3} I_i \int_0^\infty \alpha_i(\lambda) \lambda \exp(-\lambda t) d\lambda \quad \text{with} \quad (2a)$$

$$\alpha_i(\lambda) d\lambda = \frac{1}{\sigma_i^* (2\pi)^{1/2} \lambda} \exp\left[-\frac{(\ln \lambda/\lambda_{i0})^2}{2\sigma_i^{*2}}\right] d\lambda \quad (2b)$$

where λ_{i0} is the position of the maximum of $\alpha_i(\lambda)\lambda$ and $\sigma_i^* = \sigma_i(\lambda)$ is a measure for the standard deviation of the i th distribution. Each $\alpha_i(\lambda)$ is normalized so that $\int \alpha_i(\lambda) d\lambda = 1$ and $\sum I_i = 1$. A nonlinear least-squares fit of this function, convoluted with the resolution function (a sum of two Gaussians), to the spectra provides the annihilation parameters of the eqs 2a and 2b. In its version 9.0, the routine LT delivers the mean lifetimes τ_i and the mean dispersions σ_i of the corresponding lifetime distributions $\alpha_i(\tau) d\tau = \alpha_i(\lambda) \lambda^2 d\tau$, $\tau_i = \exp(-\sigma_i^{*2}/2)/\lambda_{i0}$ and $\sigma_i = \sigma_i(\tau) = \tau_i[\exp(\sigma_i^{*2}) - 1]^{0.5}$ as output.⁴³ Unconstrained three component fits have nine free floating parameters: τ_1, τ_2, τ_3 (the mean or first momentum of the lifetime distributions), $\sigma_1, \sigma_2, \sigma_3$ (the square root of the second momentum of the distributions), I_1, I_3 (the relative area below the distributions), and the time zero t_0 . The background B can be determined from the spectrum intensity at very large times $t > 70$ ns.

As an example, we present in Table 1 the results of such fits for AF 2400, performed under different assumptions. The sample was measured at 30 °C after finishing the upward and downward temperature runs and hence in equilibrium (see later). As usually, we sort the components with respect to increasing lifetimes: τ_1 , p -Ps; τ_2 , positron (e^+); and τ_3 , o -Ps. In the case of a four component analysis the o -Ps component splits up into two subcomponents which we denote here as τ_{31} and τ_{32} . The analysis “c-free” shows the parameters from an unconstrained three component fit. The analyzed parameters agree completely with the expectations. The p -Ps component, for example, which is extremely sensitive to the analysis, shows the relative intensity $F_1 = I_1/P = 25(\pm 1)\%$ ($P = I_1 + I_3$ denotes the total Ps yield) and the lifetime parameters $\tau_1 = 0.106 (\pm 0.002)$ ns and $\sigma_1 \approx 0$. Since p -Ps annihilates very rapidly mainly via self-annihilation and shows almost no interaction with matter, its lifetime should be near to the lifetime in a vacuum, 0.125 ns, without showing a distinct distribution. Recently, unconstrained LT9.0 fits to the lifetime spectra of two fluoroelastomers^{27,21} and poly(dimethylsiloxane)²⁸ delivered analogous results. In the latter polymer the Ps yield is rather higher, $P = 62\%$, which allows a very exact analysis. The spectrum analysis with discrete lifetime terms by contrast leads to a strong overestimation of τ_1 and I_1 .

The analyzed distribution in the e^+ lifetime, $\sigma_2 = 0.10$ ns and $\sigma_2/\tau_2 = 0.26$ (Table 1), may be attributed to the annihilation of positrons from different states, such as localized at local empty spaces of different size and shape and possibly at some kind of traps. An e^+ lifetime distribution ($\tau_2 = 0.363$ ns, $\sigma_2 = 0.09$ ns, $\sigma_2/\tau_2 = 0.25$) was found in the past also for Kapton, a polyimide which does not show Ps formation ($I_2 = 100\%$).^{16–18} The distribution in the o -Ps lifetime, $\sigma_3 = 2.755$ ns and $\sigma_3/\tau_3 = 0.38$ is interpreted to mirror the volume and shape distribution of the holes where o -Ps is localized. It was previously found that τ_2 and σ_2 follow closely, although not one by one, the variation of τ_3 and σ_3 as a function of temperature and pressure that may underline the role of free volume in positron annihilation.^{21,26,27}

The large number of fitting parameters can make the numerical analysis instable, particularly when the o -Ps intensity is not very high. In such cases we may introduce into the analysis two reasonable constraints: $I_1/I_3 = 1/3$ and $\sigma_1 = 0$. The results presented in Table 1 show the perfect agreement of both analyses, “c-free” and “c”, within the accuracy of the experiments. For comparison we have analyzed the spectrum assuming discrete lifetime terms for e^+ and o -Ps. The lifetime parameters from these fits and from a constrained and a free four component analysis are shown in Table 1.

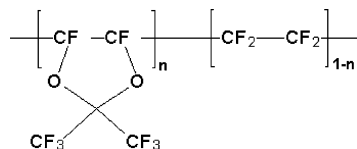


Figure 1. Repeat units of the Teflon AF copolymer.

Our results allow the following conclusions: (i) The assumption of discrete lifetime terms for *o*-Ps (τ_3) and e^+ (τ_2 , analysis “a” and “b”) leads to imperfect fits indicated by too large values for the reduced chi-square, χ^2/df , and systematic oscillations in the weighted residuals. (ii) The analysis “c” (three components, the only constraints are $I_1/I_3 = 1/3$ and $\sigma_1 = 0$) results in an excellent fit shown by the low value of χ^2/df and the statistical distribution of the residuals. The obtained fit parameters agree with those from the unconstrained analysis “c-free”. (iii) The analysis “d” (four components, either free or with the constraints $I_1/(I_{31} + I_{32}) = 1/3$ and $\sigma_1 = 0$) gives only slightly better fits than analysis “c”. We consider this as evidence that both variants “c” and “d” give approximately equal statistical fits, so it is impossible to discern the better model, at least for this polymer. So we have analyzed all spectra of our polymers by both models. One can assume that this result is the consequence of rather small Ps yield in the Teflon AF polymers. Possibly, both models could be distinguished in the case of highly porous polymers with a high Ps yield.

The unconstrained discrete four term analysis (e-discr in Table 1) show good fits with χ^2/df near 1. Compared with the analyses allowing distributions, all lifetimes shift to higher values. As usually observed in discrete term fits, the fraction of p-Ps formation, here $F_1 = 51\%$, appears too large compared with the theoretical expectation $F_1 = 25\%$.

In Figure 2, the corresponding results for the distributions of free volume for mono- and bimodal hole size distributions are plotted. We show the radius probability density functions (pdf) $n(r_h)$ calculated from $n(r_h) = -\alpha_3(\lambda) d\lambda/dr_h$, where $\alpha_3(\lambda)$ is the *o*-Ps annihilation rate pdf.^{47,7} In the case of the four component lifetime analysis the distributions $\alpha_{31}(\lambda)$ and $\alpha_{32}(\lambda)$ were weighted with their relative intensities $I_{31} = P \times F_{31}$ and $I_{32} = P \times F_{32}$ (Table 1). It is not very clear whether *o*-Ps samples holes of different size with the same probability. Frequently an increasing weight with increasing hole size is assumed.^{7,27,21} For a comparison with the theory we have therefore shown in Figure 2 the volume-weighted distributions from molecular modeling (R_{max} accessible free volume distribution for a probe molecule with the radius $r_p = 1.1$ Å, see Figure 7 in Hofmann et al.⁴⁶).

We remark again that the respective parameter χ^2/df derived from the analyses “c” and “d” do not differ very much. The distribution derived from analysis “c” of Teflon AF 2400 has a maximum at 5.4 Å and a half-width of 1.1 Å, whereas that from “d” has a dominating peak (weight 70.5/75 = 0.94) at 5.75 Å with a half-width of 1.3 Å associated with a very narrow peak at 3.8 Å (weight 4.5/75 = 0.06). Both distributions disagree with computer simulations (so-called R_{max} approximation) which show a broad peak centered at 3 Å and a flat wing up to 13 Å. There is, however, a disagreement in detail: The experimental distributions have higher mean values and narrower widths. This is also true for the four component (bimodal) analysis. The distributions for AF 1600 show the same behavior.

It can also be reminded that another simulation approach, V_{connect} used in ref 46 and elsewhere, gives two distinct peaks (bimodal size distribution of FVE), though with larger holes than are predicted by the PALS and other probe methods. For

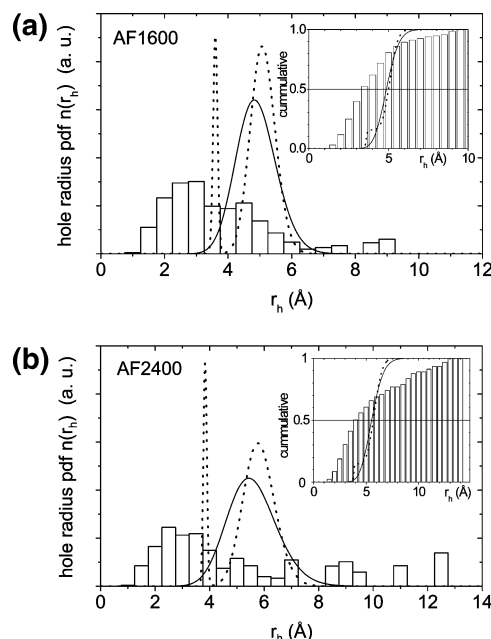


Figure 2. Hole radius probability density functions $n(r_h) = -\alpha_3(\lambda) d\lambda/dr_h$ at 30 °C. The solid and the dashed lines show the curves for a three- and a four-component analysis of the lifetime spectrum. The bars show the volume-weighted distributions from molecular modeling (R_{max} accessible free volume distribution for a probe molecule with the radius $r_p = 1.1$ Å, see Figure 7 in Hofmann et al.⁴⁶ and data are from Hofmann et al. directly and rescaled for comparison). The distributions are normalized to the unity area below the curves. The insets show the cumulative hole size distributions. Key: (a) AF 1600; (b) AF 2400.

other systems, e.g., for poly[1-phenyl-2-[*p*-(triisopropyl)phenyl]-acetylene] the agreement between the PALS data and computer simulations is much better.⁴⁶ One can assume that in real glassy polymers one encounters with some overlapping of the topologies described by the models R_{max} and V_{connect} .

The effect that both three and four component treatments of the PALS data lead to mean hole sizes larger than those from molecular dynamics calculations (in approximation R_{max} ⁴⁶) is also observed for other high free volume polymers (polyimides⁴²—poly(trimethylsilyl propyne) and for polymer sorbents.³⁴ It is likely that such a discrepancy is not accidental and is related to the mechanism of capture of positronium by free volume elements. Kirchheim et al.⁴⁸ for example, concluded that the *o*-Ps hole sizes are distinctly larger than those estimated from sample dilatation during gas sorption. These observations must be a subject of further investigations.

One important problem in calculations is how to simulate the particular response of *o*-Ps to complex holes and holes being flat or elongated. One may expect that *o*-Ps, when trapped by a larger complex hole, can move within this hole and concentrates at that part of the hole which shows the highest openness (size and three-dimensionality). Here the localized *o*-Ps finds its lowest energy level within the hole. Less open parts of this complex hole may then appear underrepresented. This possible effect is not yet considered in computer simulations. The calculations to correlate MD simulations and positronium lifetime at room-temperature we are aware of, are by Müller-Plathe et al.,⁴⁹ but it is not clear whether this gives appropriate sizes of free volume. Recently, work was performed taking into account the temperature dependence also above glass transition and hence including dynamics.⁵⁰ It might also be possible that the effective size of the *o*-Ps probe assumed in the calculations in ref 46, $r_{\text{Ps}} = 1.1$ Å, is too small to simulate correctly the

Table 2. Orthopositronium Lifetimes at Room Temperature in Teflon AF Copolymers. (Error Bars Not Given by Original Authors, Usually Less than 10% of Value)

polymer	τ_{31} (ns)	τ_{32} (ns)	atmosphere	ref
AF 1600	1.4	5.2	ambient	39
	0.68	4.7	ambient	38
		5.3	N ₂	46
AF 2400	1.4	5.5	high vacuum	this work
	1.7	6.0	ambient	38
	1.8	8.0	N ₂	46
	2.0	7.4	high vacuum	this work

localization of the Ps, a light quantum mechanical particle, in a potential well of finite width and depth. The effective size should correspond to the smallest hole size detected by o-Ps. This was estimated to $r_h \approx 1.5 \text{ \AA}$.^{22,51,52}

Since the problem of interpretation of PAL spectra via one or more orthopositronium components is very relevant for probing free volume in glassy and especially high permeability polymers and other materials, it is worthwhile to return to this subject using the LT9.0 methodology for materials with larger relative intensities of both positronium components.

Let alone the type of lifetime distribution, it is interesting to compare the longest lifetimes of amorphous Teflons AF measured in the present work and earlier publications. This is given in Table 2. It is obvious from this table that, if one takes into account the effects of oxygen quenching (measurements in air atmosphere, in a vacuum or in nitrogen atmosphere), all the works indicate that very long lifetimes are characteristic for these polymers. It means that relatively large sizes of FVE (see eq 1) should exist in the structure of amorphous Teflons AF.

Summarizing one can state that from positron lifetime alone one cannot decide the question of mono- or bimodal size distributions in high-free volume polymers. This can only be dealt with in conjunction with other techniques or methods like MD simulations. However, as it will be shown in the following paragraph, the temperature dependence can be investigated with both approaches and gives similar information.

3.2. Temperature Dependence of Positron Lifetime Spectra. Since three and four component descriptions of the PAL spectra of AF copolymers gave approximately equal results, the data accumulated at different temperatures were treated for both cases. Let us start with the three component description.

Figure 3a presents the temperature dependence of the o-Ps lifetime parameters τ_3 , σ_3 , and $I_3 = P \times F_3$ in AF 1600. This dependence closely resembles the ones obtained in the literature for numerous polymers in the temperature range below and above their glass transition temperatures. The kink in the temperature dependence of τ_3 and σ_3 occurs close to the T_g of this polymer as measured by DSC. It is interesting that above T_g the lines obtained in the heating and cooling cycles virtually coincide, which is indicative of equilibrium state of the polymer above T_g . Below T_g , some difference in lifetimes can be noted. They can be explained by a removal of the residual solvent from the rubbery polymer during the first heating run. In the polymer glass the small solvent molecules can occupy the free volume holes and reduce in this way the average hole volume detected by the o-Ps probe. This leads to a decrease in the o-Ps lifetime. When approaching the glass transition, the solvent molecules desorb from the sample, and above T_g and in the subsequent cooling run o-Ps detects the free volume structure of the pure polymer.

Comparing the slopes of the curves $\tau_3(T)$ below and above T_g with other polymers shows that the slope observed for AF 1600 does not differ noticeably from those reported for other,

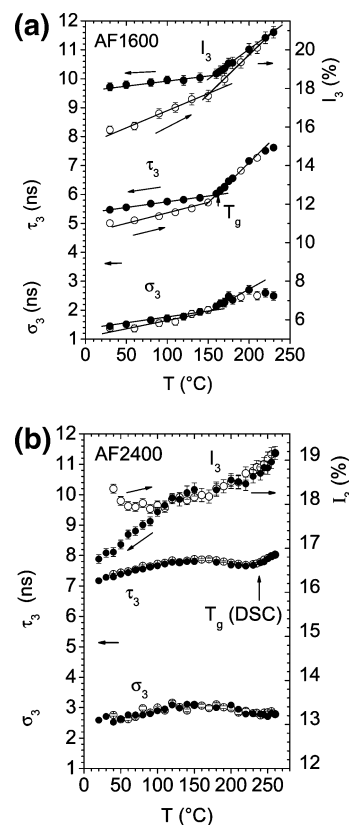


Figure 3. Lifetime parameters of o-Ps annihilation as a function of the temperature T . Shown are the mean lifetimes τ_3 , the mean dispersions σ_3 (square root of the variance the o-Ps lifetime distribution), and the relative intensities I_3 (filled circles). The open and the filled symbols come from runs with increasing and decreasing temperatures. The lines are a guide for the eyes. Key: (a) AF 1600; (b) AF 2400.

conventional glassy polymers. This result can be confirmed by much more numerous data for other polymers.

The mean dispersion of the o-Ps lifetime distribution σ_3 mirrors the density fluctuations in the amorphous polymer which have a static, frozen-in, character below T_g but a dynamic character (thermal fluctuations) above that temperature. In most polymers the ratio $\sigma_3/(\tau_3 - 0.5)$ (0.5 ns is the o-Ps lifetime limit for zero hole size) exhibits values around 0.2–0.3.^{21,22} For very flexible polymers it might be distinctly smaller. In the case of AF1600 the ratio $\sigma_3/(\tau_3 - 0.5)$ increases from 0.3 at 30 °C to 0.4 at 230 °C. These large values may be understood from the assumption that the hole size distribution is sensitive not only to thermal fluctuations but also to an inherent disorder in the random copolymer (concentration fluctuations) and changes in the conformation of this polymer (see the Discussion below).

The intensity I_3 also increases with temperature, however, similarly to τ_3 , with different slopes in the heating and cooling cycles. I_3 mirrors the Ps yield P , which is a complex function of the diffusion kinetics of positrons and free electrons, trapping and detrapping reactions of these particles with shallow or deep traps (including centers produced by the γ and fast positron radiation), and the Ps formation kinetics. Some of us observed a linear dependency between I_3 and τ_3 in thermal expansion and isothermal compression experiments for two fluoroelastomers. Arguments were given that larger holes may promote Ps formation.^{21,27}

So in different polymers various trends of the $I_3(T)$ dependencies were observed: virtual independence of T (PVA,⁵ polybutadiene,⁵³ polystyrene⁷), increase with temperature (PC, PS, PMMA,⁵⁴ polyimides⁵⁵), and even decrease (polypropy-

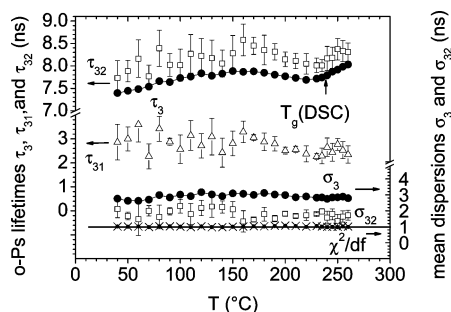


Figure 4. Comparison of the results of the three and four component analyses of lifetime spectra for AF 2400 (heating run). Filled circles: mean *o*-Ps lifetime and mean dispersion from the three component analysis, τ_3 and σ_3 . Here the error flags are smaller than the point size. Empty squares: mean and mean dispersion of the upper *o*-Ps lifetime from the four component analysis, τ_{32} and σ_{32} . Empty triangles: the lower *o*-Ps lifetime τ_{31} from the four component analysis. For reducing the scatter in the analyzed parameters, we assumed $\sigma_{31} = 0$. Compare τ_{32} and σ_{32} from the four component analysis with τ_3 and σ_3 from the three component analysis. The dots and crosses show the reduced chi-square χ^2/df of the three and four term analyses.

lene⁵⁶). Note that different behavior has been observed for the same polymers (PS). We do not discuss further this temperature dependence, though it can be noted that in the cooling cycle in the polymer which apparently contains no or very little residual solvent, the observed I_3 values are markedly higher.

Entirely different results were obtained for the temperature dependence of the more permeable polymer AF 2400—they are presented in Figure 3b. In order to remove the casting solvents, which we observed in the case of Teflon AF 1600 (see above), we have annealed this polymer in the lifetime device in a vacuum at a temperature above T_g for 1 day. Now the lifetimes τ_3 from the heating and cooling run are largely identical. Only I_3 shows a hysteresis below 100 °C. This we attributed to positron radiation effects which appear stronger in the cooling run of measurements than in the sample used for starting the heating run. This radiation effect seems to anneal out at temperatures higher than 100 °C.

Above the temperature of break (it is somewhat below T_g of this polymer from DSC) both curves coincide again, indicating that the polymer is in the equilibrium state. Above T_g the *o*-Ps lifetime behaves quite normally with a coefficient of thermal expansion of $(1/\tau_3(T_g)) d\tau_3/dT = 1.7 \times 10^{-3} \text{ K}^{-1}$, which is not as steep as for other polymers above their T_g . However, below T_g the behavior of $\tau_3(T)$ is fairly complicated showing first relatively steep increase with temperature ($\sim 0.6 \times 10^{-3} \text{ K}^{-1}$) and then a broad maximum or very weak temperature dependence.

The temperature dependences of lifetimes in AF 2400 were also considered in the approximation of a four component distribution, being equal to two *o*-Ps components and a bimodal hole size distribution. (See Figure 4.) The aim of this part of the work was to examine to what extent statistical fits will change at higher temperatures. Especially interesting is the task to examine the annihilation spectra above the corresponding T_g of both polymers, because all the high permeability polymers studied so far have glass transition temperatures above their onset of decomposition. Therefore, no information was available whether such polymers in rubbery state would keep some interesting features of high free volume polymers: the observed lifetimes above T_g are much greater than any ones reported so far for other rubbers.

As an example, we show in Figure 4 for AF 2400 the *o*-Ps lifetime parameters from the four component analysis in comparison with those from the three component analysis. The

values of χ^2/df from both fits are almost the same and very close to 1 (bottom of the Figure 4). The longer *o*-Ps component, denoted here as τ_{32} (σ_{32} , I_{32} —the intensities are not plotted), shows a behavior similar to the third term from the three component analysis, τ_3 (σ_3 , I_3). The following systematic changes between both groups of parameters can be observed in Figure 4: τ_{32} is larger than τ_3 by ~ 0.5 ns, σ_{32} is smaller than σ_3 by ~ 1 ns, and I_{32} is smaller than I_3 by $\sim 2.5\%$. This behavior can also be observed in the distributions in Figure 2. The appearance of the lower *o*-Ps lifetime τ_{31} shifts the upper *o*-Ps lifetime to larger values and narrows the distribution. τ_{31} decreases with increasing temperatures approximately linearly from 3.1 to 2.5 ns, while I_{31} stays almost constant at 2.5%. Because of the larger number of parameters in the four component analysis, the scatter in the lifetime parameters and intensities is distinctly larger than in the three component analysis. Since τ_{32} varies parallel and close to τ_3 , the qualitative conclusions from both types of analysis would not differ.

Only preliminary assumptions can be made now regarding the nature of such behavior. It can be noted that recently the temperature dependences of the positron annihilation parameters were measured for other high free volume, highly permeable polymers—poly[5-(trimethylsilyl)-2-norbornene]⁵⁷ and the so-called “polymer of intrinsic microporosity” or PIM.^{58,59} Earlier the lifetimes in poly(trimethylsilyl propyne) at different temperatures were reported.¹² In all cases, high permeability polymers revealed independence of positronium lifetimes of temperature in the glassy state. So a conclusion can be made that anomalous dependences $\tau(T)$, in contrast to conventional glassy polymers, are a feature of highly permeable polymers.

A complex character of the $\tau_3(T)$ dependence for AF 2400 observed in the present paper (see Figures 3b and 4) can be related to changes in conformation of this polymer which can occur at elevated temperatures. Quantum chemical calculations have shown⁶⁰ that the rings of 2,2-bis(trifluoromethyl)-4,5-difluoro-1,3-dioxole that form main chains in AF 2400 can exist in two conformations with different distortions of the flat shape of the ring. Their energies differ by about 10 kJ/mol. Main chains of this polymer can include also different conformations, but the energy barriers between two adjacent 2,2-bis(trifluoromethyl)-4,5-difluoro-1,3-dioxole rings are much higher (about 60 kJ/mol), so an assumption that conformation transitions occur in the main chains at 100–200 °C seems to be less probable. The changes of spatial orientation of the rings at every repeat unit can affect slightly the sizes of FVEs, as is manifested by the temperature dependence of $\tau_3(T)$. We remark here that AF 2400 exhibits extraordinary broad lifetime distributions with ratios $\sigma_3/(\tau_3 - 0.5) \approx 0.4$. These larger values occur also in the glass which shows the importance of non-thermal density fluctuations (concentration and conformational fluctuations) in this material.

For the polymers investigated here, at least a first tentative evaluation shows that if one assumes a bimodal size distribution and hence fits the data with two long lifetimes, this bimodal size distribution remains even above the caloric glass transition temperature T_g (Figure 3b). Under these assumptions, this means that a bimodal hole distribution also exists in the rubbery state. However, this seems to be surprising: a bimodal size distribution implies that holes in the polymer of the size of the minimum of the distribution (e.g., 0.4 nm for Teflon AF 1600, see Figure 2a) are either not observed or thermodynamically not stable in this polymer, even above T_g . Two speculations about this are possible. One is that this size is just the boundary for the orthopositronium between the R_{max} and the V_{connect} model; i.e.,

holes of this size are either seen as a single hole with a smaller lifetime or as larger connected holes with much longer lifetimes. The other explanation is centered around the fact, that holes of this size are thermodynamically unstable, although the reason for this is not clear yet.

There is one more point to be discussed. Obviously, intensities of the o-Ps components cannot be used directly for calculations of the number densities of the free volume holes of a given radius, since the discrete component representation is only an approximation and because density of electrons in the spur is sometimes a limiting factor. However, if once trapped o-Ps does not move from hole to hole, we might expect higher intensities of the lifetimes corresponding to holes of predominant concentration. According to simulation for AF 1600 and AF 2400, these are holes of the radius about 3 Å. However actually $I_3 < I_4$ and is about 2–3%, while $I_4 = 16\text{--}17\%$. As one of the possible explanations, this effect can be considered as a result of Ps motion, for example in a pore of a complex shape, consisting of interconnected smaller pores of different sizes, as it was discussed above in the “V-connect” model of the dynamic simulation. Further PAL investigations in combination with low-temperature gas sorption and theoretical modeling of polymer structure are considered capable of giving more insight into this problem.

Nevertheless, we may conclude that, in spite of some specific features of trapping, positron annihilation data, after appropriate treatment, can give valuable information on the pore-size distribution in systems with highly developed porosity. For example, these data give a hint on asymmetry of the distribution, information which until recently was not accessible with such more traditional methods as ^{129}Xe NMR and inverse gas chromatography.¹⁹ The role of o-Ps mobility can be further studied in comparison with sorption experiments and molecular dynamic simulations. This comparison may become still more interesting for materials with closed porosity, where possibilities of sorption methods are limited.

4. Summary

The free volume and its temperature dependence have been determined in Teflon AF 1600 and AF 2400 by positron annihilation lifetime spectroscopy in a wide temperature range (25–260 °C) including both the regions of glassy and rubbery states of both copolymers. Large lifetimes were observed both at room and at elevated temperatures. Three or four component descriptions of lifetime spectra gave approximately equal fits for both polymers implying bimodal or monomodal free volume size distributions. The temperature dependence of lifetimes reveals interesting differences between the two materials. Teflon AF 1600 shows a regular behavior with a change in slope of the o-Ps lifetime and hence free volume vs temperature around T_g , whereas the unusual behavior of Teflon AF 2400 can be related to reversible isomerization of dioxolane rings that affects the chain packing in this polymer with rather rare appearance of tetrafluoroethylene units in the main chains.

Acknowledgment. The authors thank Prof. D. Hofmann and Dr. M. Heuchel for helpful discussions and providing data for Figure 2. Dr. J. Pionteck (Dresden) is acknowledged for the characterization of polymers by DSC.

References and Notes

- (1) Schrader, D. M.; Jean, Y. C. *Positron and Positronium Chemistry*; Elsevier: Amsterdam, 1988.
- (2) Jean, Y. C.; Mallon, P. E.; Schrader, D. M. *Principles and Application of Positron and Positronium Chemistry*; World Scientific: Singapore, 2003.
- (3) Bartos, J. In *Encyclopedia of Analytical Chemistry*; Meyers, R. A., Ed.; Wiley: Chichester, U.K., 2000; p 7968.
- (4) Yampolskii, Yu. P.; Shantarovich, V. In *Materials Science of Membranes for Gas and Vapor Separation*; Yampolskii, Y., Pinnau, I., Freeman, B. D., Eds.; Wiley: Chichester, U.K., 2006; p 191.
- (5) Kobayashi, Y.; Zheng, W.; Meyer, E. F.; McGervey, J. D.; Jamieson, A. M.; Simha, R. *Macromolecules* **1989**, *22*, 2302.
- (6) Hristow, H. A.; Bolan, B.; Yee, A. F.; Xie, L.; Gidley, D. W. *Macromolecules* **1996**, *29*, 8507.
- (7) Liu, J.; Deng, Q.; Jean, Y. C. *Macromolecules* **1993**, *26*, 7149.
- (8) Tao, J. J. *Chem. Phys.* **1972**, *56*, 5499.
- (9) Eldrup, M.; Lightbody, D.; Sherwood, J. N. *J. Chem. Phys.* **1981**, *63*, 51.
- (10) Jean, Y. C. *Microchem. J.* **1990**, *42*, 72–102.
- (11) Yampolskii, Yu. P.; Shantarovich, V. P.; Chernyakovsky, F. P.; Kornilov, A. I.; Plate, N. A. *J. Appl. Polym. Sci.* **1993**, *47*, 85.
- (12) Consolati, G.; Genco, I.; Pegoraro, M.; Zanderighi, L. *J. Polym. Sci. Pol. Phys.* **1997**, *34*, 357.
- (13) Okamoto, K.; Tanaka, K.; Ito, M.; Kita, H.; Ito, Y. *Mater. Sci. Forum* **1995**, *175–178*, 743.
- (14) Hougham, G.; Zhang, Q.; Jean, Y. C. *Polym. Prepr. (Am. Chem. Soc., Div. Polym. Chem.)* **1998**, *39*, 871.
- (15) Winberg, P.; Desitter, K.; Dotremont, C.; Mullens, S.; Vankelcom, I. F. J.; Maurer, F. H. J. *Macromolecules* **2005**, *38*, 3776.
- (16) Dlubek, G.; Hübner, C.; Eichler, S. *Nucl. Instrum. Methods Phys. Res. B* **1998**, *142*, 191–202.
- (17) Dlubek, G.; Eichler, S.; Hübner, C.; Nagel, C. *Phys. Status Solidi A* **1999**, *174*, 313.
- (18) Dlubek, G.; Eichler, S.; Hübner, C.; Nagel, C. *Nucl. Instrum. Methods Phys. Res. B* **1999**, *149*, 501.
- (19) Golemme, G.; Nagy, J. B.; Fonseca, A.; Algieri, C.; Yampolskii, Yu. P. *Polymer* **2003**, *44*, 5039.
- (20) Wang, Y.; Inglefield, P. T.; Jones, A. A. *J. Polym. Sci., Polym. Phys.* **2002**, *40*, 1965.
- (21) Dlubek, G.; Wawryszczuk, J.; Pionteck, J.; Goworek, T.; Kaspar, H.; Lochhaas, K. H. *Macromolecules* **2005**, *38*, 429–437.
- (22) Kilburn, D.; Wawryszczuk, J.; Dlubek, G.; Pionteck, J.; Hässler, R.; Alam, M. A. *Macromol. Chem. Phys.* **2005**, *206*, 818.
- (23) Bohlen, J.; Kirchheim, R. *Macromolecules* **2001**, *34*, 4210.
- (24) Deng, Q.; Jean, Y. C. *Macromolecules* **1993**, *26*, 30.
- (25) Dlubek, G.; Saarinen, K.; Fretwell, H. M. *J. Polym. Sci., Polym. Phys.* **1998**, *36*, 1513.
- (26) Dlubek, G.; Supej, M.; Bondarenko, V.; Pionteck, J.; Pompe, G.; Krause-Rehberg, R.; Emri, I. J. *J. Polym. Sci., Polym. Phys.* **2003**, *41*, 3077.
- (27) Dlubek, G.; Gupta, A. S.; Pionteck, J.; Krause-Rehberg, R.; Kaspar, H.; Lochhaas, K. H. *Macromolecules* **2004**, *37*, 6606.
- (28) Dlubek, G.; De, U.; Pionteck, J.; Arutyunov, N. Y.; Edelmann, M.; Krause-Rehberg, R. *Macromol. Chem. Phys.* **2005**, *206*, 827.
- (29) Srithawatpong, R.; Peng, Z. L.; Olson, B. G.; Jamieson, A. M.; Simha, R.; McGervey, J. D.; Maier, T. R.; Halasa, A. F.; Ishida, H. *J. Polym. Sci., Polym. Phys.* **1999**, *37*, 2754.
- (30) Schmidt, M.; Maurer, F. H. J. *Polymer* **2000**, *41*, 8419.
- (31) Wang, Y. Y.; Nakanishi, H.; Jean, Y. C.; Sandreczki, T. C. *J. Polym. Sci., Polym. Phys.* **1990**, *28*, 1431.
- (32) Hirade, T.; Maurer, F. H. J.; Eldrup, M. *Radiat. Phys. Chem.* **2000**, *58*, 465.
- (33) Shantarovich, V. P.; Goldanskii, V. I. *Hyperfine Interact.* **1998**, *116*, 67.
- (34) Shantarovich, V. P.; Suzuki, T.; Djourelou, N.; Shimazu, A.; Gustov, V. W.; Kevdina, I. B. *Acta Phys. Polym., A* **2005**, *107*, 629.
- (35) Resnick, P. R.; Buck, W. H. In *Modern Fluoropolymers: High Performance Polymers for Diverse Applications*; Scheirs, J., Ed.; Wiley: Chichester, U.K., 1997; p 397.
- (36) Nemser, S. M.; Roman, I. A. US Patent 5,051,114, 1991.
- (37) Pinnau, I.; Toy, L. G. *J. Membr. Sci.* **1996**, *109*, 125.
- (38) Alentiev, A. Yu.; Yampolskii, Yu. P.; Shantarovich, V. P.; Nemser, S. M.; Plate, N. A. *J. Membr. Sci.* **1997**, *126*, 123–132.
- (39) Davies, W. D.; Pethrick, R. A. *Eur. Polym. J.* **1994**, *30*, 1289.
- (40) Shantarovich, V. P.; Kevdina, I. B.; Yampolskii, Yu. P.; Alentiev, Yu. A. *Macromolecules* **2000**, *33*, 7453–7466.
- (41) Alentiev, A. Yu.; Shantarovich, V. P.; Merkel, T. C.; Bondar, V. I.; Freeman, B. D.; Yampolskii, Yu. P. *Macromolecules* **2002**, *35*, 9513–9522.
- (42) Kruse, J.; Kanzow, J.; Rätzke, K.; Faupel, F.; Heuchel, M.; Frahn, J.; Hofmann, D. *Macromolecules* **2005**, *38*, 9638.
- (43) Kansy, J. *Nucl. Instrum. Methods Phys. Res. A* **1996**, *374*, 235.
- (44) Kansy, J. LT for Windows, Version 9.0, Inst. of Phys. Chem. of Metals, Silesian University, Bankowa 12, PL-40-007 Katowice, Poland, March 2002, private communication.
- (45) Schrader, D. M.; Usmar, S. G. In *Positron Annihilation in Fluids*; Sharma, S. C., Ed.; World Scientific: Singapore, 1988; p 215.

- (46) Hofmann, D.; Entrialgo-Castano, M.; Lebre, A.; Heuchel, M.; Yampolskii, Yu. P. *Macromolecules* **2003**, *36*, 8528.
- (47) Gregory, R. B. *J. Appl. Phys.* **1991**, *70*, 4665.
- (48) Bohlen, J.; Wolff, A.; Kirchheim, R. *Macromolecules* **1999**, *32*, 3766.
- (49) Schmitz, H.; Müller-Plathe, F. *J. Chem. Phys.* **2000**, *112*, 1040.
- (50) Racko, D.; Chelli, R.; Cardini, G.; Bartos, J.; Califano, S. *Eur. Phys. J. D* **2005**, *32*, 289.
- (51) Ito, Y. *Mater. Sci. Forum* **1995**, 175–178, 627.
- (52) Jasinska, B.; Koziol, A. E.; Goworek, T. *Acta Phys. Polym., A* **1999**, *95*, 557.
- (53) Bartos, J.; Bandzuch, P.; Sausa, O.; Kristiakova, K.; Kristiak, J.; Kanaya, T.; Jenninger, W. *Macromolecules* **1997**, *30*, 6906.
- (54) Xie, L.; Gidley, D. W.; Hristow, H. A.; Yee, A. F. *J. Polym. Sci., Polym. Phys.* **1995**, *33*, 77.
- (55) Shantarovich, V. P.; Suzuki, T.; He, C.; Ito, Y.; Yampolskii, Yu. P.; Alentiev, Yu. A. *Radiat. Phys. Chem.* **2005**, *73*, 45.
- (56) Uedono, A.; Kawano, T.; Tanigawa, S.; Ban, M.; Kyoto, M.; Uozumi, T. *J. Polym. Sci., Polym. Phys.* **1997**, *35*, 1601.
- (57) Finkelshtein, E.; Makovetskii, K.; Gringolts, M.; Rogan, Yu.; Golenko, T.; Starannikova, L.; Yampolskii, Yu. P.; Shantarovich, V.; Suzuki, T. *Macromolecules* **2006**, *39*, 7022.
- (58) De Miranda, R. L.; Kruse, J.; Rätzke, K.; Faupel, F.; Fritsch, D.; Abetz, V.; Budd, P.; Selbie, J.; McKeown, N.; Ghanem, B. *Phys. Status Solidi Rapid Res. Lett.* **2007**, *5*, 190.
- (59) Shantarovich, V.; Suzuki, T.; Ito, Y.; Kondo, K.; Yu, R. S.; Budd, P. M.; Yampolskii, Yu. P.; Berdonosov, S.; Eliseev, A. *Phys. Status Solidi C*, in press.
- (60) Tokarev, A. V.; Bondarenko, G. N.; Yampolskii, Yu. P. *Polym. Sci. Ser. A* **2007**, *49*, 909–920.

MA071563Z